MAUSAM, **67**, 2 (April 2016), 357-376

551.501.8 : 551.553.21 (540)

Characteristics of movement of low level clouds associated with onset / wet spells of northeast monsoon of Indian sub-continent as derived from high resolution INSAT OLR data

B. AMUDHA, Y. E. A. RAJ and R. ASOKAN

Regional Meteorological Centre, India Meteorological Department, Chennai – 600 006, India

(*Received 7 November 2014, Accepted 16 March 2015*)

e mail : amudha2308@gmail.com

सार – भारतीय भूस्थैतिक उपग्रहों की श्रृंखला से उत्तरी हिंद महासागर और दक्षिण प्रायद्विपीय भारत (SPI) के ऊपर से व्युत्पन्न बहिर्गामी दीर्घ तरंग विकिरण (OLR) का उपयोग करके उत्तर पूर्वी मॉनसून (NEM) के लक्षणों का अध्ययन किया गया है। वर्ष 2000-2012 की अवधि के 1° × 1° ग्रिडिड उच्च विभेदन OLR आँकड़ों का उपयोग करके उत्तर पूर्वी मॉनसून के आगमन के चरण के दौरान दक्षिण पूर्व से उत्तर पश्चिम दिशा की ओर भूमध्यरेखीय मेघ क्षेत्र की दिशा के विरोधामासी लक्षणों को दोहराया गया है। आँकडों के अध्यारोपित प्रतिध्वनि के अध्ययन से मॉनसून के आरंभ होने की तारीख से तटीय तमिलनाडु के बड़े भाग में 180 Wm^{-2} से कम OLR मानों का होना तथा दक्षिण पूर्व से SPI की ओर मेघ बनने के साथ वर्षा का साथ साथ आरंभ होना स्पष्ट है। OLR के ट्रैड मीन्स इस संदर्भ की पुष्टि करते हैं। बहुत लम्बे समय तक शुष्क दौर के बाद होने वाले NEM के सक्रिय दौर के दौरान, OLR परिरेखाओं से मेघ के दक्षिण से उत्तर की ओर बढने की पुनरावृत्ति तथा इसके संभावित कारणों को इस शोध पत्र में बताया गया है। SPI में NEM की वापसी के चरण के दौरान श्रीलंका के क्षेत्र में मौजूद सक्रिय मॉनसून स्थिति को इस क्षेत्र में 230 Wm^{-2} से कम OLR परिरेखाओं की गति के साथ दर्शाया गया है।

ABSTRACT. Characteristics of the northeast monsoon (NEM) have been studied utilising the outgoing long wave radiation (OLR) data derived over the north Indian Ocean and south peninsular India (SPI) from the series of Indian geostationary satellites. The contrasting feature of movement of the equatorial cloud zone from southeast to northwest direction during the onset phase of NEM has been reiterated using 1° × 1° gridded high resolution OLR data for the period 2000-2012. Presence of OLR values less than 180 Wm^{-2} over a large part of coastal Tamil Nadu on the date of onset and the simultaneous commencement of rainfall with clouding approaching SPI from southeast is clear from the study of superposed epoch analysis of the data. Triad means of OLR also substantiate this inference. During active spells of NEM which succeed prolonged dry spells, replication of the south to north movement of clouding by the OLR contours and the plausible reasons for such a movement have been brought out. The active monsoon situation existing over Sri Lankan region during the withdrawal phase of NEM over SPI is demonstrated with the depiction of the movement of OLR contours less than 230 Wm^{-2} over the region.

Keywords – Northeast monsoon, Onset, Satellite, Outgoing long wave radiation, Active spell, Dry spell, Withdrawal, Superposed epoch analysis.

1. Northeast monsoon

Indian monsoon comprises of two distinct seasonal circulations (Ramage, 1971), a winter outflow from a cold continental anticyclone which is the northeast monsoon (NEM) and a summer inflow into a continental heat low emerging as the southwest monsoon (SWM). The Indian NEM is a smaller spatial scale monsoon confined to parts of south peninsular India (SPI) which sets in after the withdrawal of SWM from most parts of India. Sometimes, there is no clear-cut indication of the withdrawal of SWM and the onset of the winter NEM over SPI as one tends to merge with the other (Das, 1986). The duration of NEM is for three months, October, November and December (OND) occasionally spilling over to January of the next calendar year, generally in one-third of the years. NEM is associated with the seasonal reversal of surface and lower tropospheric southwesterly (SW) winds prevalent during the SWM season of June to September to northeasterly (NE) winds which set in over the Indian region in October (IMD, 1973). The passage of the equatorial trough over SPI from north to south is associated with reversal of lower level winds from SW to NE. The subsequent increase in rainfall (RF) over the SPI is taken as the setting in of NEM. Various characteristic features of the NEM and its teleconnections have been widely researched [Raj (1992, 1996, 1998a&b and 2003); Jayanthi and Govindachari (1999); Suresh and Raj (2001); Khole and

De (2003); Kripalani and Pankaj Kumar (2004); Balachandran *et al*. (2006); Pankaj Kumar (2006); Zubair and Ropelewski (2006); Asokan and Balachandran (2008); Raj and Geetha (2008); Geetha and Raj (2009); Nayagam *et al*. (2009); Geetha (2011)]. The above studies have explored the latent and causative aspects which manifest and make the NEM behave as it does every year. The quest to understand the hitherto unknown dimensions and complexities of NEM continues.

The normal date of onset of NEM over coastal Tamil Nadu (CTN) is 20th October with a standard deviation (SD) of 7-8 days. The withdrawal dates for 1991-2000 were determined by Raj (2003) as around 27th December with a SD of 13-14 days. While the onset date re-determined for the period 1901-2000 by Geetha and Raj (2015) using a larger RF data set of stations along CTN remained unchanged, the mean withdrawal date has got extended by three days to 30 December. Tamil Nadu (TN) is the major beneficiary of NEM. Nearly 48% (438 mm) of its annual RF of 914 mm is received during NEM season (Raj, 2012). The monthly normal RF values over TN during October, November and December are 180.2, 170.0 and 88.0 mm respectively.

With the advent of the satellite era since 1960s, researchers have been using the data from remote sensing platforms to understand various features of the monsoons. The basic purpose of meteorological satellites is to observe clouds (Kelkar, 2007). Innumerable derived products apart from the satellite cloud imageries help in reiterating objectively the movement of monsoon clouds and synoptic scale atmospheric phenomena hitherto inferred based on climatological characteristics. Raj *et al.* (2007), based on INSAT (Indian National Satellite) outgoing long wave radiation (OLR) data of 2.5°×2.5° resolution for the 12 year period 1987-1991 and 1993-1999 (data unavailable for 1992) and other synoptic data including upper air winds, showed the existence of a contrasting movement of low level clouds from the equatorial zone of Bay of Bengal (BoB) from southeast (SE) to northwest (NW) direction into the CTN and south coastal Andhra Pradesh (CAP). The movement of clouds was not from NE direction from which the low level winds blow which was also the reason behind the nomenclature NEM. Possible causes behind the movement of clouds from south to north have been elucidated by Raj *et al., loc.cit*. During active NEM, the meridional wind which is northerly in the lower levels veers to southerlies whereas strength of zonal easterlies increases by three times that in the lower level at the time of onset. Hence, there is a large amount of moisture flux towards the coast which increases from south to north. Raj *et al. loc.cit.* have highlighted using OLR variability over ocean, some of the significant characteristics of NEM which have till now been documented based only on RF over land, position and movement of the equatorial trough and cloud zone over the Indian peninsula.

The main aim of the study is to utilise OLR data of higher resolution (1° × 1°) than that used by Raj *et al. loc. cit*., to analyse for a period of 13 years (2000-12), some features of NEM and substantiate their earlier observation that the movement of clouding is from SE to NW direction during onset of NEM. That a similar cloud movement observed at the time of onset of NEM is conspicuous during every wet (active) spell of monsoon activity following a prolonged dry (weak) spell is a new result that emerged from this in-depth study of the OLR variability and has been appropriately emphasised. The present work is also construed as a significant validation reiterating the reliability of Indian satellite based OLR data retrievals in reproducing the characteristics of NEM. The variations in OLR during the onset phase of NEM and signals of periodicity of NEM from OLR pentads of October have been explored and highlighted. The signatures of the active NEM phase over Sri Lanka indicated by the occurrence of RF during withdrawal of NEM from SPI have been brought out from the OLR analysis.

The forthcoming Section 2 is an overview of the methodology used for computation of OLR using satellite data. Section 3 deals with the data used. Section 4 is a brief discussion on the significance of using an optimal threshold value of OLR as 230 Watts/square metre (Wm^{-2}) associated with NEM cloudiness. Section 5 dwells upon how the analyses and calculations were carried out. Salient features of NEM inferred from OLR data form part of Section 6 under results and discussions. Overall comments have been provided in Section 7 and inferences are listed in Section 8.

2. Methodology for OLR computations

Indian geostationary satellites beginning from INSAT-1A to 2B had visible (VIS, 0.55 to 0.75 μm) and infra-red (IR, 10.5 to 12.5 μm) channels in the Very High Resolution Radiometer (VHRR) onboard which measure the radiant flux (power) of electromagnetic radiation emitted by the earth-atmosphere system in specific wavelengths of the spectrum. From INSAT-2E onwards up to the present INSAT-3D, water vapour (WV, 5.7 to 7.1 μm) channel became an essential component of the VHRR. Satellites sense the temperatures of the surface of the earth / clouds in the field of view of the sensors. Earth absorbs solar radiation incident on it and emits terrestrial radiation in the long wavelength or IR spectral region of 3-100 μm. Maximum intensity of emitted radiation is at 10μm and the satellite maps the IR radiances in the band

of 10.5 to 12.5 μm. IR channel gives a thermal image of the earth-atmosphere in terms of OLR. Data from the IR channel is also converted to temperature, using the concept of brightness temperature.

Meteorological parameters are derived using data from satellite-based sensors operating in the IR region so that information is available both during day and night. Since the long wave ranges from 3 to 100 μm, the observed narrow band radiance is mapped to broadband for the entire range by physical/statistical/empirical techniques using linear regression developed from the theoretical apriori radiative transfer calculations (Rao *et al*., 1989). The OLR from the earth observed at the top of the atmosphere (ToA) is an important parameter in the earth-atmosphere radiation budget. High values of OLR are associated with high radiative temperature of matter on or near the earth's surface and lack of intense convective clouds in the free atmosphere. On the other hand, low values of OLR are associated with low radiative temperatures of cold cloud tops (Weickmann *et al*., 1985). OLR responds to variations in cloudiness (both height and frequency of occurrence) and surface temperature. When the area seen by the satellite is cloud-free, it records the sea surface temperature over oceans and the land surface temperature otherwise. Arkin *et al*. (1989) have explained that over the tropical oceans, because of the relatively stable surface temperature, OLR variations are due almost entirely to changes in the distribution of cloudiness and hence are related to changes in precipitation. IR channel is primarily sensitive to the temperature of the lowest visible surface (*i.e.*, either land/ocean or cloud top), but the measured OLR at the ToA is also sensitive to the vertical distribution of temperature and moisture (Mahakur *et al*., 2013). Most satellite based techniques are built on the hypothesis that brighter (colder) clouds in visible (IR) imagery are associated with higher precipitation (Rao *et al*., *loc.cit*.). When the surface of the earth is masked by clouds over the area, then the temperature of the cold cloud top is sensed by the satellite. Hence, lesser OLR indirectly means higher chances of precipitation and so OLR is regarded as a proxy parameter for convective activity.

OLR is calculated in terms of the brightness temperatures (T_r, in K) of the earth's surface being observed and measured with a resolution of 8 km per pixel by the IR-channel of the geostationary satellites up to INSAT-3A and with 4 km resolution in INSAT-3D at present. Large differences in T_r sensed by the satellite are produced by the varying distribution of moisture in the vertical layers over different locations. If the atmosphere contained absolutely no moisture, T_r would be equal to the surface black body temperature. In a deep moist layer, T_r decreases. So, a dense and moisture-packed cloud will have cold cloud tops. The T_r obtained over the Indian Ocean region at three-hourly intervals, *viz*., 0000, 0300, 0600, 0900, 1200, …, 2100 UTC over particular coordinates are averaged to compute the flux temperature T_f (in K) and in turn to calculate OLR in Wm^{-2} from σT_f^4 where σ is the Stefan-Boltzmann constant(5.67×10^{-8} $Wm^{-2}K^{-4}$). Daily mean OLR value of each point in the grid of 1°×1° Long./Lat. resolution is then obtained. OLR values available for a given place, eight times a day provides higher credibility to the daily average (Kelkar, 1993) computed for a specific grid point coordinate. For a nadir view, the regression equation is given by

$$T_f = T_r(a + T_r b) \tag{1}$$

where '*a*' and '*b*' are constants (Ohring *et al.*, 1984) which depend upon the response function of the filter-sensor system onboard and is satellite instrument-specific. For zero zenith angle, the coefficients are a =1.1889 and b =0.000989/K (Rao *et al., loc.cit*.). With increasing zenith angles (α), both '*a*' and '*b*' decrease in magnitude and

$$T_f = T_r(a + T_r b\cos\alpha) \tag{2}$$

Knowing T_r of each individual pixel in an imagery and using Eqn. (2), T_f is calculated. The mean OLR of a 1°×1° Long./Lat. box is computed using the values of T_r and T_f of that many pixels in the grid box under consideration. Results from the validation of the statistical algorithms implemented for OLR retrievals over the Indian region based on radiances mapped by the INSAT-1B satellite have been documented (Rao *et al*., *loc.cit*). Improvements based on statistical techniques are carried out continuously to increase the data reliability and accuracy in the algorithms / calibration constants applied for retrieval of OLR from satellite radiometers. The algorithms up to the year 2007 for retrieval of OLR data from IR radiances are those used for the INSAT first generation satellite series. During 2008-2009, a processing system with a new application software using a Genetic Algorithm (GA) technique (Randhir *et al*., *2007*) in a radiative transfer model, incorporating the radiances from the WV channel in addition to IR for estimating OLR was implemented. The OLR data of the 13 year period 2000-2012 used in this study is from two Indian geostationary satellites INSAT-1D and Kalpana-1.

3. Data

The following data sets have been utilised in this study.

3.1. The re-determined dates of onset and withdrawal of NEM (Geetha & Raj, 2015) as given in Table 1.

TABLE 1

Re-determined dates of onset, withdrawal and duration of Indian northeast monsoon (NEM) for the period 2000-01 to 2012-13

Year	Date & month of		Duration of NEM (days)
	onset	withdrawal	
2000-01	03 Nov	02 Jan	61
2001-02	15 Oct	01 Jan	79
2002-03	09 Oct	12 Dec	65
2003-04	19 Oct	08 Dec	51
2004-05	18 Oct	16 Dec	60
2005-06	11 Oct	21 Dec	72
2006-07	17 Oct	14 Dec	59
2007-08	19 Oct	07 Jan	81
2008-09	12 Oct	21 Dec	71
2009-10	29 Oct	26 Dec	59
2010-11	29 Oct	06 Jan	70
2011-12	24 Oct	10 Jan	79
2012-13	18 Oct	11 Jan	85

(*Source* : Geetha and Raj, 2015)

3.2. The daily mean OLR data in text format for the period 1st October to 31st January for 13 years (2000-12) at 1°×1° Long./Lat. grid resolution over the area 60°-100° E and 0°-30° N (Fig. 1) lying over parts of Indian peninsular region and the North Indian Ocean (NIO) was obtained from the archives of National Data Centre (NDC), Pune and the Satellite Meteorology Division, India Meteorological Department (IMD), New Delhi.

3.3. IR satellite imageries from IMD, New Delhi, available for the period 2005-12, for the dates of onset and withdrawal as mentioned in 3.1 above.

3.4. Daily rainfall (DRF) data for the period 1st October to 31st January, 2000-12 for 27 stations of CTN and 2 stations of CAP. The geographical locations of the stations are depicted in Fig. 2.

3.5. Long term DRF normals of all the 29 stations as per 3.4 above derived from the data base of the period 1951-2000 from NDC, Pune (IMD, 2010).

3.6. RF expressed as percentage departures from normal (PDN) for the NEM season (1st October to 31st December) for TN (Fig. 3) from Regional Meteorological Centre (RMC), Chennai. The definition of RF PDN = $\left(\frac{A-N}{N}\right)\times 100$, where, A = actual RF and N is the normal RF for a NEM season.

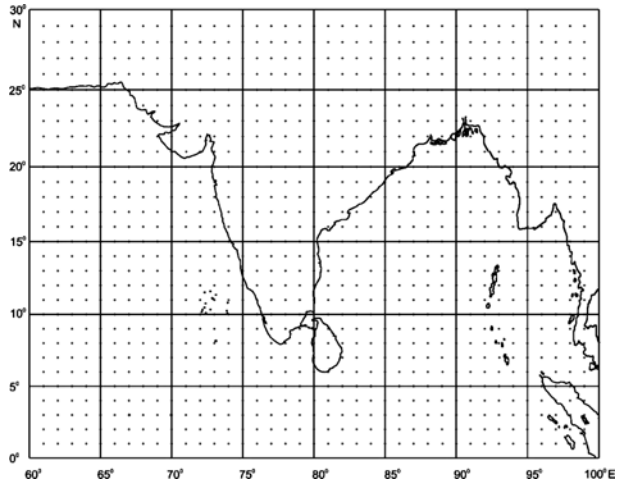

Fig. 1. Area of study and grid points at which OLR data is available

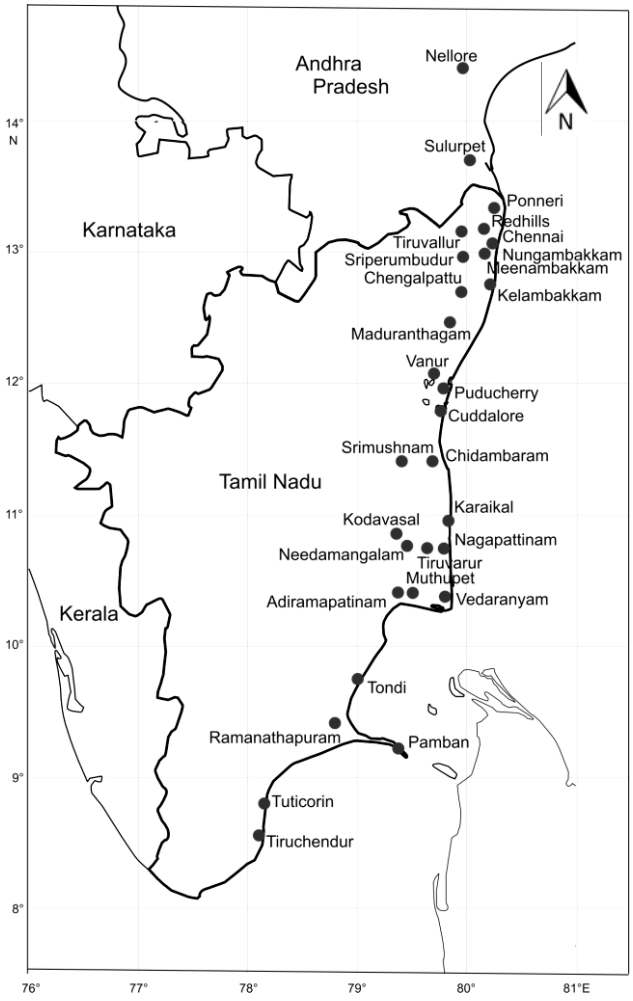

Fig. 2. Geographical locations of the 29 stations of coastal Tamil Nadu and Andhra Pradesh considered in the study

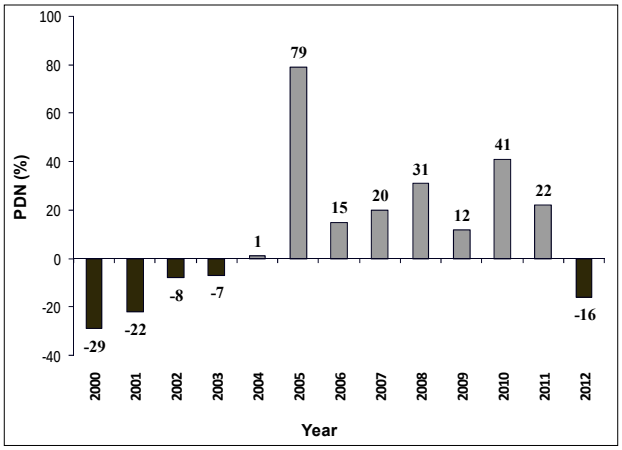

Fig. 3. Yearwise percentage departure of rainfall from normal for the northeast monsoon season of Tamil Nadu for 2000-12

3.7. Cyclonic disturbances (CDs) that occurred during 2000-12 over BoB/NIO (IMD, Cyclone e-Atlas, 2011) and coincided with the commencement of a wet spell of NEM after a prolonged dry spell.

4. Optimal threshold value of OLR associated with NEM cloudiness

As elucidated in Section 2, OLR is taken as a proxy for convection, clouding and rainfall. In this study, we propose to analyse the pattern of movement of clouds over BoB and SE Indian peninsula during onset of NEM and at the beginning of a fresh rain spell after a prolonged dry phase of NEM. To proceed further, it is necessary to arrive at a threshold value of OLR which will indicate NEM clouding.

In recent years, IMD has enlarged the criteria for deciding the onset of SWM over Kerala by including several parameters representing the monsoon flow pattern. One such criterion is that INSAT derived OLR value should be below 200 Wm^{-2} in the box confined by latitudes between 5°-10° N and longitudes 70°-75° E as a requisite for declaring onset of SWM over Kerala (IMD, 2008). The same approach has been adopted by Joseph *et al*., 2006 in their study on onset of SWM. In a similar manner, a threshold value for NEM clouding can also be identified. While doing so, considering the fact that the clouds associated with NEM are much shallower than those of SWM with the former known to be reaching only up to a height of 3-4 km, a higher threshold of OLR value equal to 230 Wm^{-2} was adopted by Raj *et al*. (2007), to delineate clouding associated with NEM onset. In this paper also, OLR value of 230 Wm^{-2} has been taken as the best and optimal value to represent NEM clouding and to define the northern limit of the equatorial cloud zone (ECZ).

5. Analysis and computations

5.1. *OLR data*

The OLR data for the region of interest (40 Long. × 30 Lat. grid) and period of study (as mentioned in Section 3.2) was processed. Fortran programming language, GrADS (Grid Analysis and Display System) software and other standard statistical packages were used for data processing, computations and pictorial representations. Figures depicting the spatial variability of OLR over the region of study (Fig. 1), were generated for all days for which data was available, to analyse the spatial and temporal OLR variability prior to, during and after onset of NEM.

OLR data of all the 13 years for a given grid point were averaged with reference to the yearly onset dates of NEM utilising the concept of the well known compositing technique called superposed epoch analysis (SEA), (Panofsky & Brier, 1968). The spatial distribution of OLR was derived for 15 days prior to and after the onset of NEM. Spatial profiles of OLR by computing triad (three days) and pentad (five days) means of the 13 years data were generated. Day-to-day OLR anomalies in October were also computed.

5.2. *Rainfall data*

Utilising the DRF data of 29 stations, the spatial distribution and strength of NEM activity on a daily basis in terms of RF were assessed over the region comprising of CTN and parts of south CAP (Fig. 1). This was done as per the classifications followed by IMD describing the RF distribution spatially over a region as dry, isolated, scattered, fairly widespread and widespread. The strength of NEM is termed either as Weak, Normal, Active or Vigorous as per IMD nomenclature.

The DRF data of all the 13 years (2000-12) for the 29 stations was analysed. The mean RF of a day was computed based on the number of stations for which RF data was available. Using the DRF normals (IMD, 2010) of these coastal stations, the normal rainfall (NRF) expected for each day (1st October to 31st January) for the region of study, *viz*., CTN and CAP was computed. The ratio of actual to NRF was calculated for every day of the 13 year period. Thereafter, the strength and spatial distribution of NEM were determined for each day and year of the study period. The data thus sequentially generated as explained above, was further analysed to identify periods of wet (active) spells which followed prolonged dry (weak) spells of NEM RF activity and are listed in Table 2(a) for each year.

TABLE 2(a)

Duration and period of wet spells of northeast monsoon preceded by long dry spells from 2000-01 to 2012-13

S. No.	Year	Spell				Whether	
		Dry		Wet			
		Duration (days)	Period	Duration (days)	Period	CD was present in the BoB / NIO	S to N movement was observed
1.	2000-01	21	6-26 Dec	3	27-29 Dec	Yes	*
2.	2001-02	15	3-17 Dec	10	18-27 Dec	No	Yes
3.	2002-03	11	22 Nov - 2 Dec	9	3-11 Dec	No	Yes
4.	2003-04	5	23-27 Nov	4	28 Nov - 1 Dec	No	Yes
5.	2004-05	9	5-13 Dec	2	14-15 Dec	No	Yes
6.	2005-06 (a)	7	14-20 Nov	8	21-28 Nov	Yes (2)	*
7.	2005-06 (b)	4	6-9 Dec	5	10-14 Dec	Yes	*
8.	2006-07	12	28 Nov - 9 Dec	3	10-12 Dec	No	#
9.	2007-08	6	8-13 Dec	2	14-15 Dec	No	Yes
10.	2008-09	24	26 Oct - 18 Nov	12	19-30 Nov	Yes (2)	*
11.	2009-10	8	5-12 Dec	6	13-18 Dec	Yes	*
12.	2010-11 (a)	6	10-15 Dec	3	16-18 Dec	No	&
13.	2010-11 (b)	7	22-28 Dec	1	29 Dec	No	&
14.	2011-12	15	8-22 Nov	7	23-29 Nov	Yes	*
15.	2012-13 (a)	14	9-22 Nov	3	23-25 Nov	Yes	*
16.	2012-13 (b)	21	5-25 Dec	5	26-30 Dec	No	Yes

CD - Cyclonic Disturbance, BoB - Bay of Bengal, NIO - North Indian Ocean, S - South, N - North
* - Influence of the CD in BoB/IO areas close to south CTN and CAP, in terms of rainfall activity would be present with movement of clouds from east towards west and hence not considered for analysing the S to N movement
# - OLR data not available for the days of wet spell
& - OLR data available for the days of wet spell but of doubtful quality

TABLE 2(b)

Details of cyclonic disturbances that occurred over Bay of Bengal / North Indian Ocean and coincided with the commencement of a wet spell of northeast monsoon

S. No.	Year	Period of CD	Type of CD	Origin	Dissipation
1.	2000	23-28 Dec	VSCS	Central parts of south BoB	East central Arabian Sea
2.	2005	20-22 Nov	D	SW BoB	Gulf of Mannar and neighbourhood
3.	2005	28 Nov - 2 Dec	CS Bazz	SE BoB	SW and adjoining west central BoB off North TN-south AP coasts
4.	2005	6-10 Dec	CS Fanoos	BoB	South TN and neighbourhood
5.	2008	13-17 Nov	CS Khaimuk	SE and adjoining SW BoB	Rayalaseema and neighbourhood
6.	2008	25-27 Nov	CS Nisha	Sri Lanka and neighbourhood	North TN and adjoining areas of south interior Karnataka and Rayalaseema
7.	2009	10-15 Dec	CS Ward	SW and adjoining SE BoB	Sri Lanka
8.	2011	26 Nov - 1 Dec	DD	Comorin area and neighbourhood	West central Arabian Sea
9.	2012	17-19 Nov	DD	East central BoB	-

D : Depression, DD : Deep Depression, CS : Cyclonic Storm, VSCS : Very Severe Cyclonic Storm

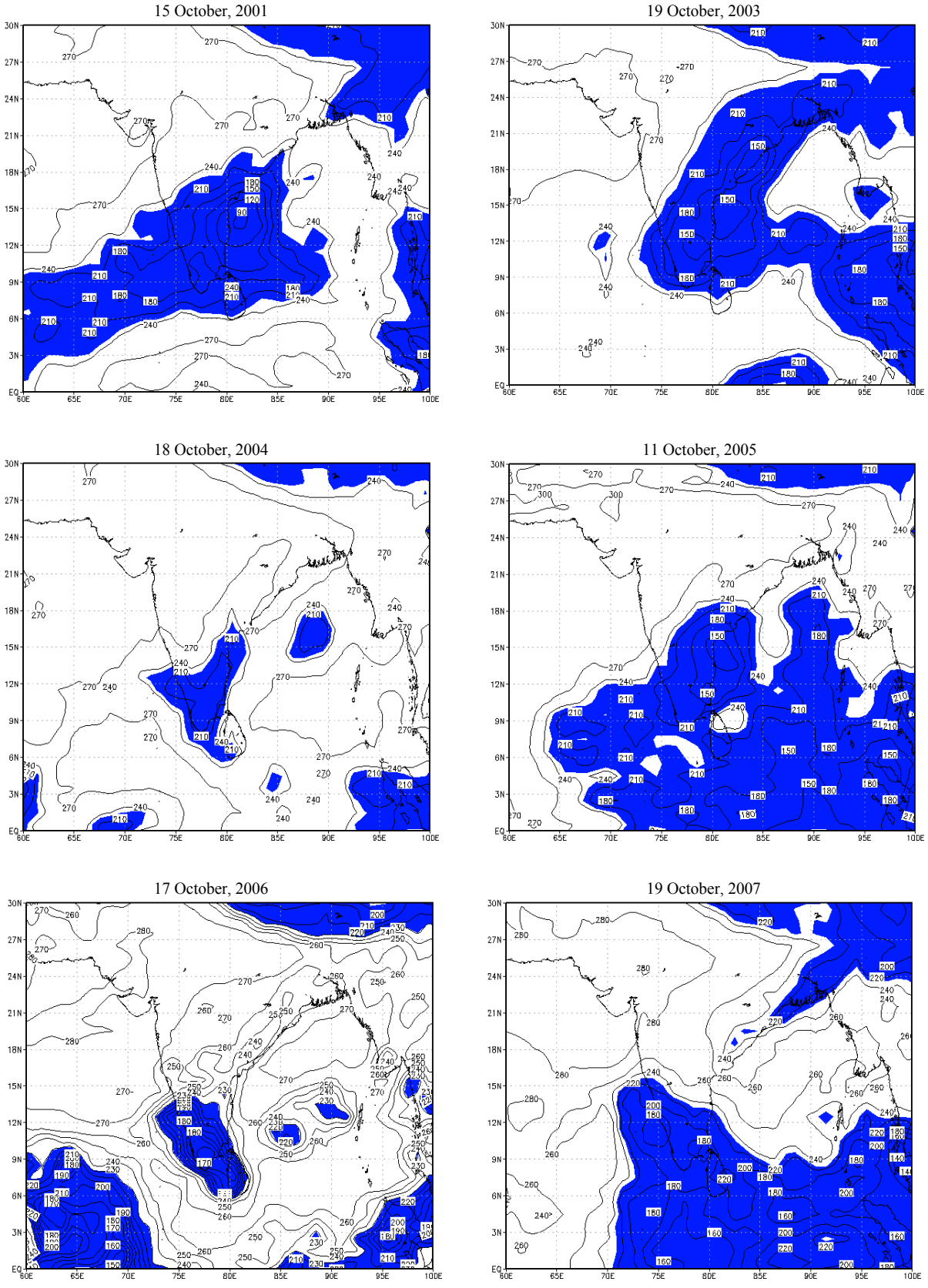
15 October, 2001
19 October, 2003
18 October, 2004
11 October, 2005
17 October, 2006
19 October, 2007

Fig. 4. (*contd*.)

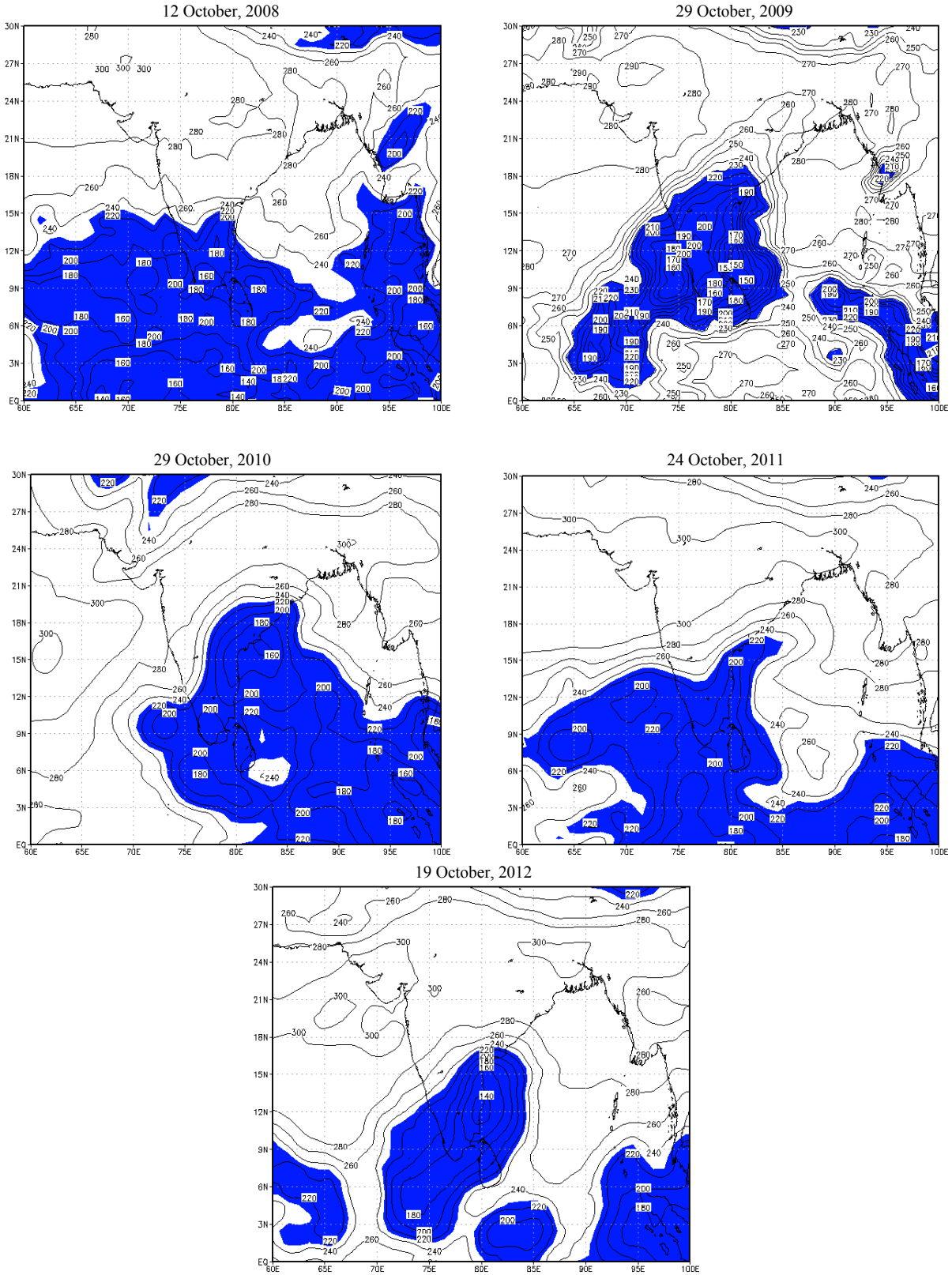

Fig. 4. Spatial variation of OLR on the onset dates (given above the images) of northeast monsoon for each year of the period 2000-12 (OLR data for onset dates of 3 November, 2000 and 9 October, 2002 not available, shaded areas : OLR ≤ 230 Wm^{-2})

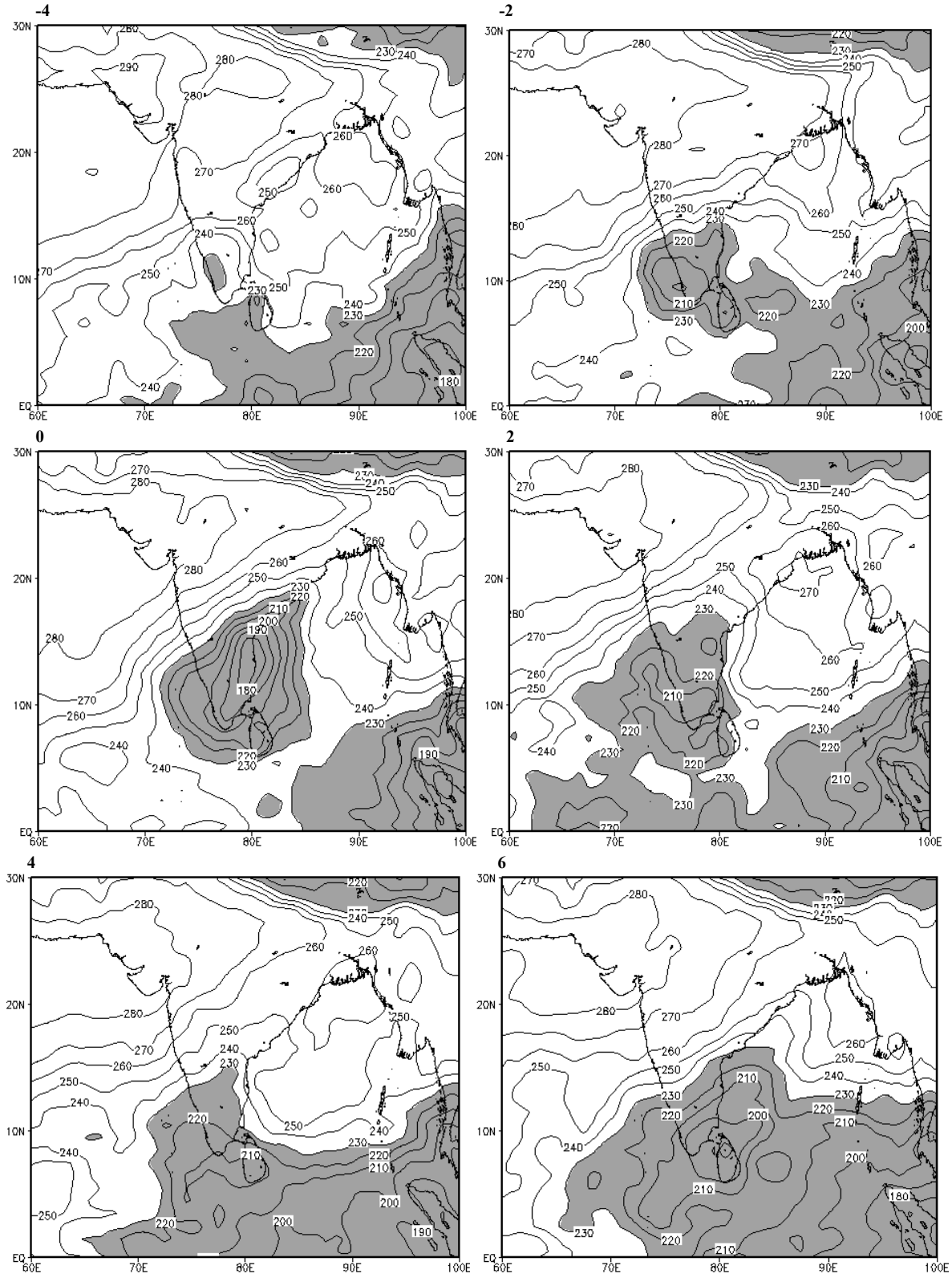

Fig. 5. Spatial variability of mean OLR data for -4, -2, 0, 2, 4 & 6 days with respect to northeast monsoon onset days based on superposed epoch analysis (Data used : 2000-12) (*shaded areas* : OLR ≤ 230 Wm^{-2})

5.3. *Occurrence of cyclonic disturbances*

Table 2(b) contains the details of cyclonic disturbances (CDs) that occurred over BoB / NIO (IMD, Cyclone e-Atlas, 2011) and coincided with the commencement of a wet spell of NEM after a prolonged dry spell. The duration, type, origin, landfall (if occurred) and dissipation of 9 CDs have been provided in Table 2(b). In our subsequent analysis, we have excluded such wet spells when the revival of NEM over CTN was owing to the approaching CD from BoB. It is well known that CDs forming over south BoB during NEM season frequently take a NW-ly course and strike CTN / CAP (Raj, 2012) and in such instances the clouding associated with the movement of the CDs also exhibits SE to NW movement. Such cases which are as anticipated have been excluded from the analysis.

5.4. *Variability in OLR during wet and dry spells*

The spatial variation of OLR with reference to such (a) dates of commencement of wet spells over two (diad) or three (triad) days and (b) dry spells prior to these wet spells was also computed for each corresponding year. The purpose behind such averaging over 2 or 3 days is to reduce noise and to effect temporal smoothing by taking into consideration that DRF is cumulated over 24 hours and frequently a single spell of RF may get distributed over two calendar days. The spatial variation of OLR in SPI and adjoining Sri Lankan region at the time of NEM withdrawal over CTN was also analysed.

In the forthcoming sections, results that emerged out of the analysis as described above are discussed.

6. Results and discussion

6.1. *Yearwise spatial variation of OLR on the day of NEM onset*

During the onset phase of NEM, the ECZ by and large moves from south / SE towards NW as shown by Raj *et al*., *loc.cit.* utilising OLR data of 1987-99. This pattern of movement has been specifically reiterated for the NEM season of 2009 (Geetha *et al*., 2010) by a study of the movement of cloud echoes captured by the Doppler Weather Radar of Chennai. The onset of NEM, by definition, is always associated with a wet spell (convective clouding and low values of OLR) and the succeeding season is interspersed with wet and dry spells up to the time of withdrawal (Raj, 2012). As mentioned in Section 5 above, pictures were generated using daily OLR data to study the daily spatial variation of OLR. In Fig. 4 we present the spatial distribution of OLR over the region of study for the dates of onset of NEM for each year 2001-12 (OLR data for the onset dates of the years 2000 and 2002 were not available). Several interesting inferences could be drawn from the detailed analysis of Fig. 4 and some are enumerated below.

(*i*) On the date of NEM onset, in the years 2001, 2005, 2008, 2009, 2010 and 2011, the northern limit of OLR $\leq$ 230 Wm^{-2} (NLOLR230) extends north of 15° N and in some other years beyond 18° N.

(*ii*) In several years, another spell of clouding as delineated by NLOLR230 is observed in the NE region.

(*iii*) In between the clouding associated with NEM in SPI and clouding over NE India, a clearly defined large cloud free zone with OLR values between 230 and 260 Wm^{-2} indicating absence of clouding is observed. Only in 2004 and 2006, on the date of onset, clouds are relatively less over SPI. In seven out of eleven years, values of OLR much less than 180 Wm^{-2} are observed on the date of onset in some grid points of SPI indicating the presence of very intense convection.

The inferences reveal that clouding generally increases from north to south (up to 10.5° N) and further the NEM zone is clearly delineated by NLOLR230 with a large area of cloud free zone over northern India at the time of NEM onset. Barring one or two years, clouding is present and widely distributed over BoB region adjoining SPI. The lowest values of OLR observed over NIO / SPI / CTN, range between 90 and 210 Wm^{-2} indicative of very intense to normal RF activity on the dates of onset of NEM. In addition, in almost all the years except 2009 and 2011, the remnant cloud clusters of SWM in higher latitudes beyond 27° N, especially over NE India are observed on the date of onset of NEM. An examination of the thermal IR imageries (not shown here) from Kalpana-1 satellite indicated the spatial extent of clouding observed on the dates of onset of NEM during the years 2005, 2007, 2009 and 2011.

6.2. *Mean spatial variability of OLR prior to and after onset of NEM*

6.2.1. *Daily spatial variation of OLR by superposed epoch analysis*

SEA (Section 5.1) was performed on the daily mean OLR data to derive the daily spatial and temporal variation for 15 days prior to and after the date of onset. The date of onset of each year (Table 1) is considered as the '0^{th}' day and the calendar dates preceding the onset dates are assigned as -1, -2, -3,… and succeeding dates assigned 1, 2, 3,… (*loc.cit.*). All such OLR values of the 0^{th} day for each grid across the 13 years (2000-12), were thus arranged and averaged as corresponding to the OLR mean variability on the 0^{th} day. Similar averaging was

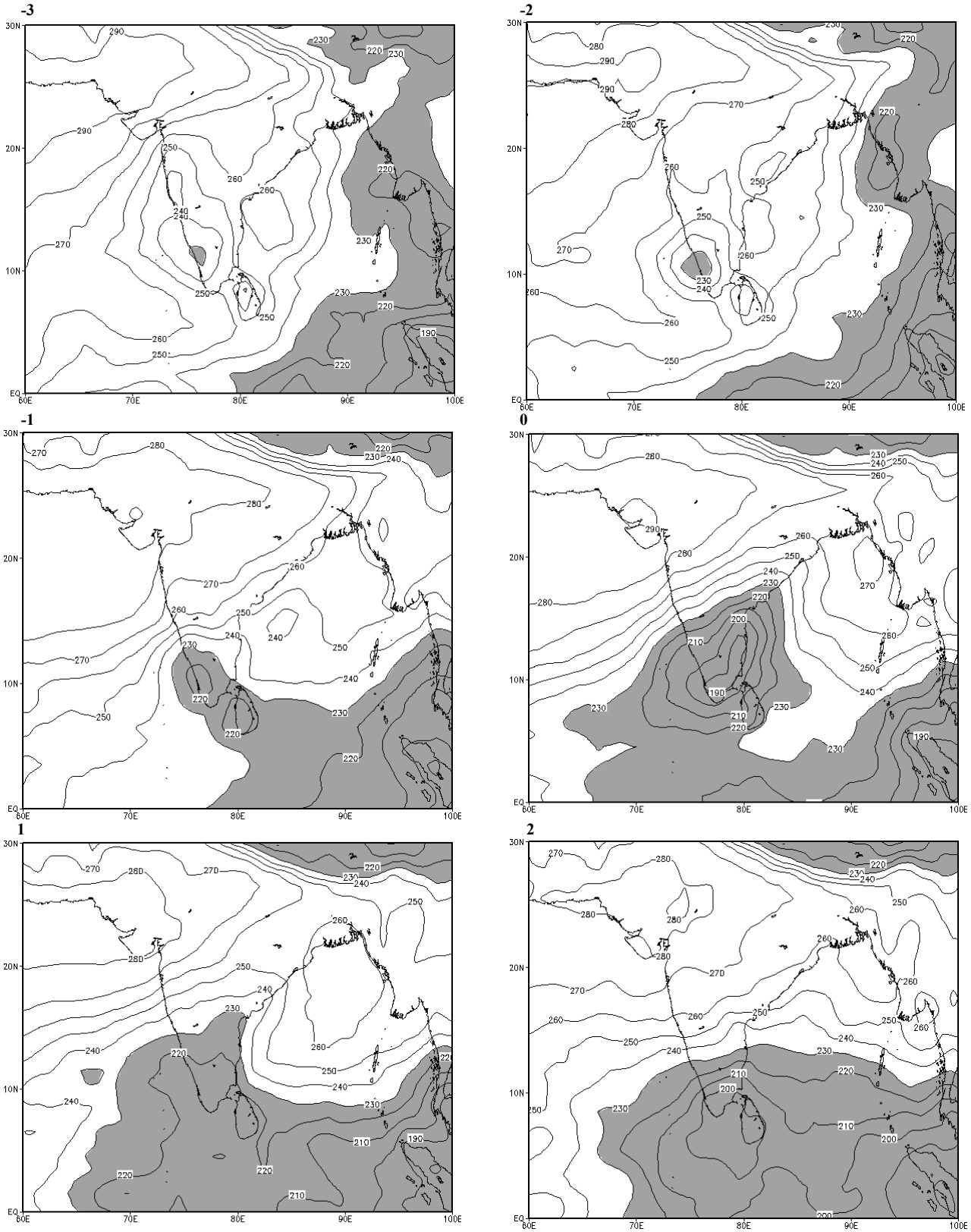

Fig. 6. Mean spatial variability of OLR at triads of -3, -2, -1, 0, 1, 2 with reference to the yearly onset date of northeast monsoon
Data used: 2000-12 (shaded areas : OLR ≤ 230 Wm^{-2})

done for the rest of the -15 to +15 days with reference to the onset date of NEM for each of the 13 years.

The average spatial variability of OLR on -4, -2, 0, 2, 4 and 6 days with reference to the date of onset is depicted in Fig. 5. The gradual advancement of OLR isopleths from SE to NW from -4 days to the 0^{th} day and hence the movement of clouding associated with onset of NEM is clearly observed from the figure. The existence of values of OLR $\leq$ 230 Wm^{-2} beyond 27° N and between 80-100° E in Fig. 5 indicating RF activity over the higher latitudes of NE Indian region and the onset phase of NEM over SPI is also evident. Four days prior to the onset day, almost all of SPI is cloud free with OLR $\leq$ 230 Wm^{-2} observed over Kerala alone, indicating that SWM has not yet withdrawn from the State. However, cloud mass with OLR $\leq$ 180 Wm^{-2} approaches SPI from 70° to 100° E and extends up to 8° N. Two days prior to onset, contours of OLR $\leq$ 200 Wm^{-2} engulf south CTN and Kerala while the NLOLR230 extends up to 13° N. On the date of onset *i.e.*, 0^{th} day, values of OLR $\leq$ 180 Wm^{-2} are present over north CTN and south CAP indicating the intense rainfall activity associated with the onset of NEM over that region. The axis of the lowest OLR is tilted towards NE direction, *i.e.*, the ridge of the OLR contours lies along the east coast of India indicating that for a given latitude, clouding is maximum near the coast.

There is another region of significant clouding over SE BoB. Branching of cloud clusters into two portions, one covering and the other approaching land from BoB is evident. Two days after the onset, contours of OLR $\leq$ 230 Wm^{-2} extend up to 15° N and envelop parts of CAP indicating slightly lower rainfall activity compared to that of the date of onset. Four days after, contours of OLR $\leq$ 230 Wm^{-2} have extended only up to south and interior TN and parts of Kerala indicating active NEM conditions over these areas. Six days hence, NLOLR230 extends up to 16° N. Fig. 5 authenticates that the advancement of low level clouds over BoB is from SE to NW towards SPI and not from NE on the eve of NEM.

6.2.2. *Triad variations in OLR using superposed epoch analysis*

As discussed in Section 6.2.1, spatial and temporal changes in the daily OLR manifested during the onset phase of NEM could be understood from the SEA performed on the OLR data with reference to the date of onset. The discussions in Section 6.2.1 were based on the specific days prior to and after onset each year, though averaged for 13 years. Sometimes, it is preferable to average the OLR distribution over 2-3 days to reduce noise inherent in spatial distributions for a given day. Keeping this in mind, mean spatial variations of OLR have been derived using SEA with reference to the onset date, for triads of -3, -2, -1, 0, 1 & 2 (Fig. 6). The OLR values observed at the specified grid points on the seventh, eighth and ninth days prior (*i.e.*, -7,-8,-9) to the onset date of NEM and averaged, constitute the '-3 triad'. Similarly, '-2 triad' and '-1 triad' represent the averaged OLR values of -4, -5, -6 days and -1, -2, -3 days from the date of onset of NEM respectively. The '0 triad' (0, 1, 2) denotes averaging of OLR values of the date of onset, the first and second days after onset. Similarly, '1 triad' (3, 4, 5) and '2 triad' (6, 7, 8) denote similar such averaging of OLR values observed respectively on the days mentioned in brackets, from the date of onset.

It is seen from the OLR distribution of '-3 triad' (Fig. 6) that near cloud free conditions exist over SPI covered by contours of OLR between 230 and 260 Wm^{-2} with a small stretch over central Kerala having OLR $\leq$ 230 Wm^{-2}. This feature is reasonably consistent with the withdrawal of SWM from most parts of India by the pentad 11-15 October. Presence of OLR $\leq$ 190 Wm^{-2} in east BoB indicates perhaps the genesis phase of NEM prior to its onset over SPI. Similar pattern is observed during '-2 triad' also with the contours of OLR $\leq$ 230 Wm^{-2} occupying a slightly larger area of Kerala, while the clouding over east BoB persists as observed in '-3 triad'. Three days prior to the onset (-1 triad) of NEM, OLR $\leq$ 230Wm^{-2} persistent over Kerala merges with the cloud clusters of east BoB and covers south CTN up to 10° N. The onset triad (0 triad) denotes the clear displacement of the OLR contours towards NE, covering SPI with the NLOLR230 reaching up to 18° N and surrounding CAP. Presence of values of OLR $\leq$ 190 Wm^{-2} indicates comparatively an intense RF activity within five days of onset of NEM with OLR $\leq$ 230 Wm^{-2} extending up to 17° N and covering entire SPI. Eight days from the date of onset, rainfall activity over SPI up to 13° N is evident. From the above triad analysis also, it is confirmed that the movement of clouds is gradually from SE towards north / NW / NE direction. Pentad compositing during the onset phase also yielded similar results reiterating the above conclusion, though the figures have not been included here. In addition, during the pentads of 21-25 and 26-30 October, day-to-day negative OLR anomalies in the range -6 to -4 Wm^{-2} were observed indicative of the onset phase of NEM in the south peninsular region.

6.3. *Spatial OLR variability during the active and weak spells of NEM*

It is well established that the NEM season is characterised by wet (active) spells of RF interspersed with light and dry (weak) spells in between. Most often, during the entire NEM season, the activity of the NEM

would be suppressed or inhibited for a few days which might extend to weeks on rare occasions due to complex imbalances in thermodynamical parameters of the atmosphere (IMD, 1973 and Raj, 1996). Subsequently, under favourable synoptic conditions, a wet (active) spell of RF would commence after a prolonged dry (weak) spell. Sometimes, sporadic instances of formation of CDs in the BoB herald the revival of NEM activity after a lull.

Dry spell is defined as one when the NEM RF is nil or isolated over CTN and CAP. During the NEM season, RF spells extend up to 3-4 days; spells exceeding 4 days are very much smaller in number (about 20%), though, spells even longer than 10 days have occurred. There are sometimes long spells with little or no rain, which on rare occasions have been even longer than those of the non-monsoon months (IMD, 1973).

In the present analysis, during the NEM season for the study period 2000-12, 181 spells comprising of Dry (no rain) - 86 (47%); Light (little rain) - 32 (18%) and Active (significant rain) - 63(35%) were observed. Out of the 63 active spells, those which persisted for four days and above are 39 (62%) and those which were less than four days are 24 (38%). Spells exceeding 10 days were 14 (22%). Clearly, this statistics also reveals that 2000-12 had more number of active spells (35%), than that stated (about 20% of the spells of 1875-1951) in IMD, 1973 because of the epochal RF activity of the period 2004-11 which had positive RF PDNs. During 2000-12, out of 1196 days (October-403, November-390, December-403), NEM activity was weak, normal, active and vigorous on 55%, 28%, 12% and 6% of the occasions respectively. It is seen from Table 2(a) that during 2000-12, duration of dry spells varied from 4 to 24 days. Dry spells greater than 20 days (nearly three weeks) were observed in three NEM seasons, 2000-01 [6-26 Dec (21 days)]; 2008-09 [26 Oct - 18 Nov (24 days)]; 2012-13 [(5-25 Dec (21 days)].

One of the major objectives of this study is to test and demonstrate the postulate that, every year, during instances of active spells commencing after prolonged dry spells of NEM, the movement of the clouds is from south/SE to NW analogical to the pattern of cloud movement observed in the onset phase of NEM. Hence, as mentioned in Section 5.2 above, such wet spells that followed prolonged dry spells were listed for each year in Table 2(a). There had been 16 such spells with the years 2005, 2010 and 2012 having two spells each while the other years experienced one such spell.

On nine instances as listed in Table 2(b), in six years, *viz*., 2000(1), 2005(3), 2008(2), 2009(1), 2011(1) and 2012(1), the dates of origin, persistence and dissipation of CDs in BoB / NIO have coincided either with a dry spell period over SPI when the CD was in BoB or a wet spell period over SPI associated with the CD's movement inland. For example, in the year 2005, a dry spell of 7 days (14-20 November) was followed by a wet spell of 8 days (21-28 November) [Table 2(a)]. During the period 20-22 November, southwest (SW) BoB was affected by a CD which formed near 7.5° N / 85.2° E, moved westwards, crossed both the east and west coast of Sri Lanka and emerged in the Gulf of Mannar and dissipated at about 9° N. The NEM revived on 21 November in association with the movement of this CD in a westnorthwest (WNW) direction. So, the wet spell of 21-28 November 2005 has been excluded from the analysis in view of reasons as elaborated in Section 5.3. In addition, during 2005 [Table 2(b)], three CDs (20-22 November, 28 November-2 December, 6-10 December) contributed towards two wet spells. Similarly, there were two CDs (13-17 and 25-27 November) in BoB, in the year 2008, one during the dry spell period of SPI (26 October-18 November) and the other heralding the wet spell (19-30 November). Hence, out of the 16 spells listed in Table 2(a), 7 wet spells have been excluded from the analysis of OLR variability during active and weak spells due to the presence of CDs in BoB / NIO [Table 2(b)].

There were three spells in two years 2006 and 2010 for which the OLR variability on the days of dry and wet spells was contrary to expected results and hence had to be excluded from the analysis of whether south to north movement was observed. In the case of 2006, a prolonged dry spell (28 November-9 December) preceded a wet spell of 3 days (10-12 December). However, daily mean OLR data was not available for the period since 7th December and hence the variability could not be verified. On other days when OLR data for December was available, the dry spell was less than 4 days and could not be considered as it would not be purely representative of a clear dry regime of NEM. In the case of the year 2010, while there were two dry spells in December (10-15, 6 days; 22-28, 7 days) preceding their corresponding wet spells (16-18, 3 days; 29, 1 day), values of OLR > 230 Wm^{-2} over SPI in the range of 250-270 Wm^{-2} were observed during the wet spell, indicating non-rainy days whereas RF has been recorded by rain gauges along CTN. Perhaps, on these days, missing data of a few hours due to non-availability of satellite pass data (which could not be confirmed) in the averaging of the OLR data of a day could have led to this error in the daily mean OLR values available. Interestingly, such limitations in statistically retrieved data from modern remote sensing observing systems can give rise to errors / systematic bias in the data sets. The OLR data retrievals used particularly in this study are from two different VHRRs onboard the satellites. Caution has been exercised in interpretation of the features of NEM, from

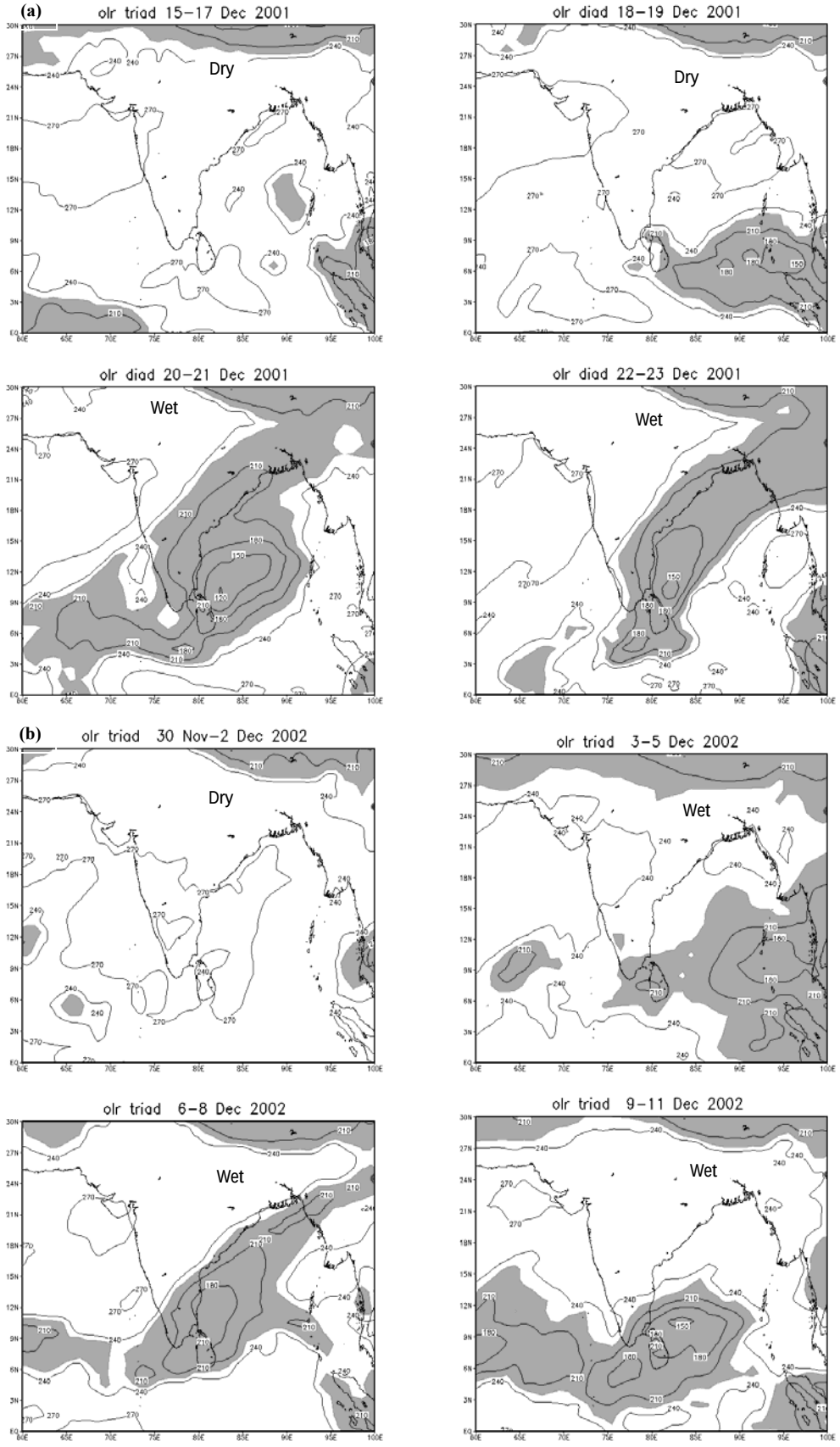
(a)
olr triad 15–17 Dec 2001
Dry
olr diad 18–19 Dec 2001
Dry
olr diad 20–21 Dec 2001
Wet
olr diad 22–23 Dec 2001
Wet
(b)
olr triad 30 Nov–2 Dec 2002
Dry
olr triad 3–5 Dec 2002
Wet
olr triad 6–8 Dec 2002
Wet
olr triad 9–11 Dec 2002
Wet

Fig. 7. (*Contd*.)

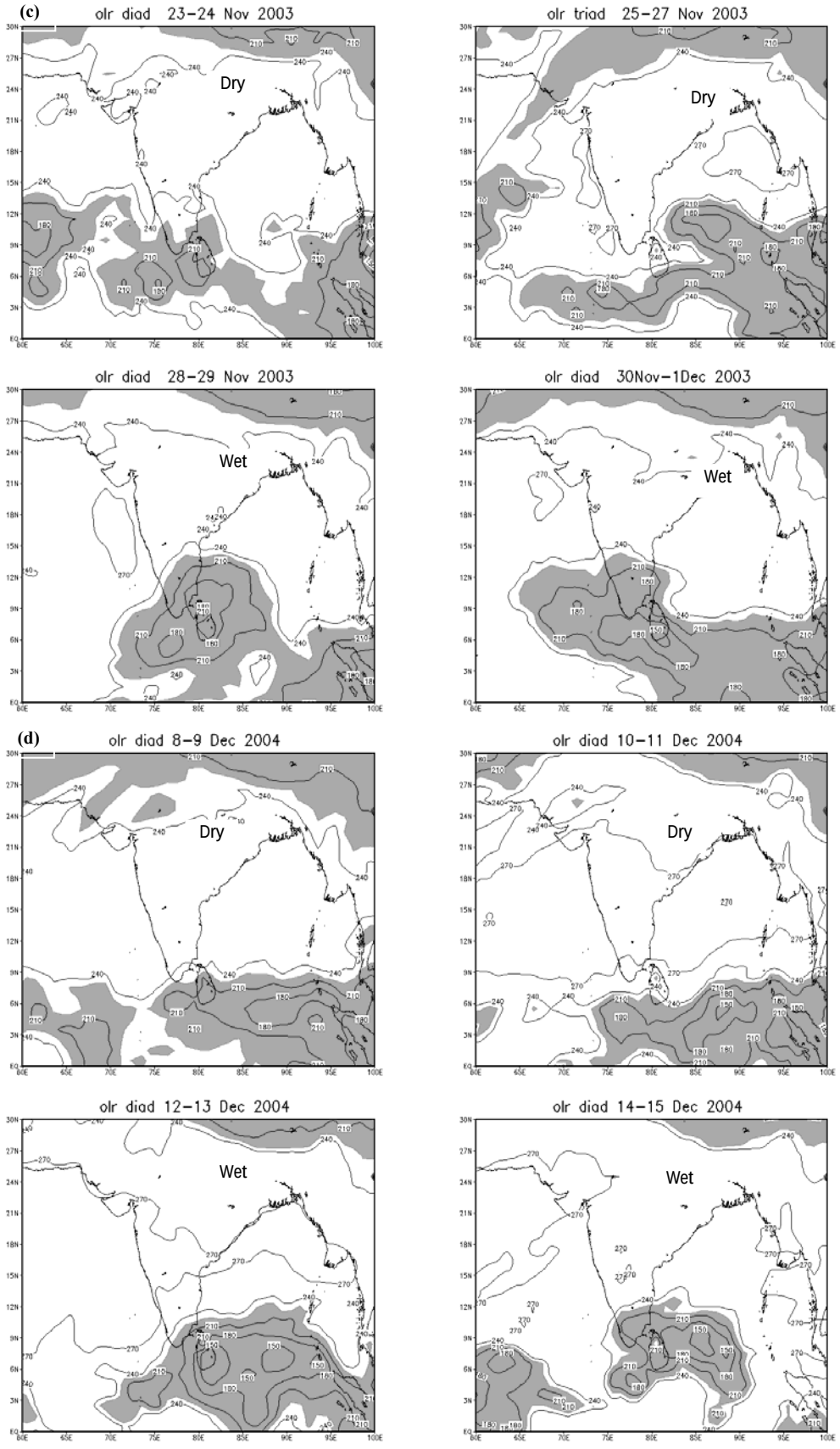
(c)
olr diad 23–24 Nov 2003
Dry
olr triad 25–27 Nov 2003
Dry
olr diad 28–29 Nov 2003
Wet
olr diad 30Nov–1Dec 2003
Wet
(d)
olr diad 8–9 Dec 2004
Dry
olr diad 10–11 Dec 2004
Dry
olr diad 12–13 Dec 2004
Wet
olr diad 14–15 Dec 2004
Wet

Fig. 7. (*Contd.*)

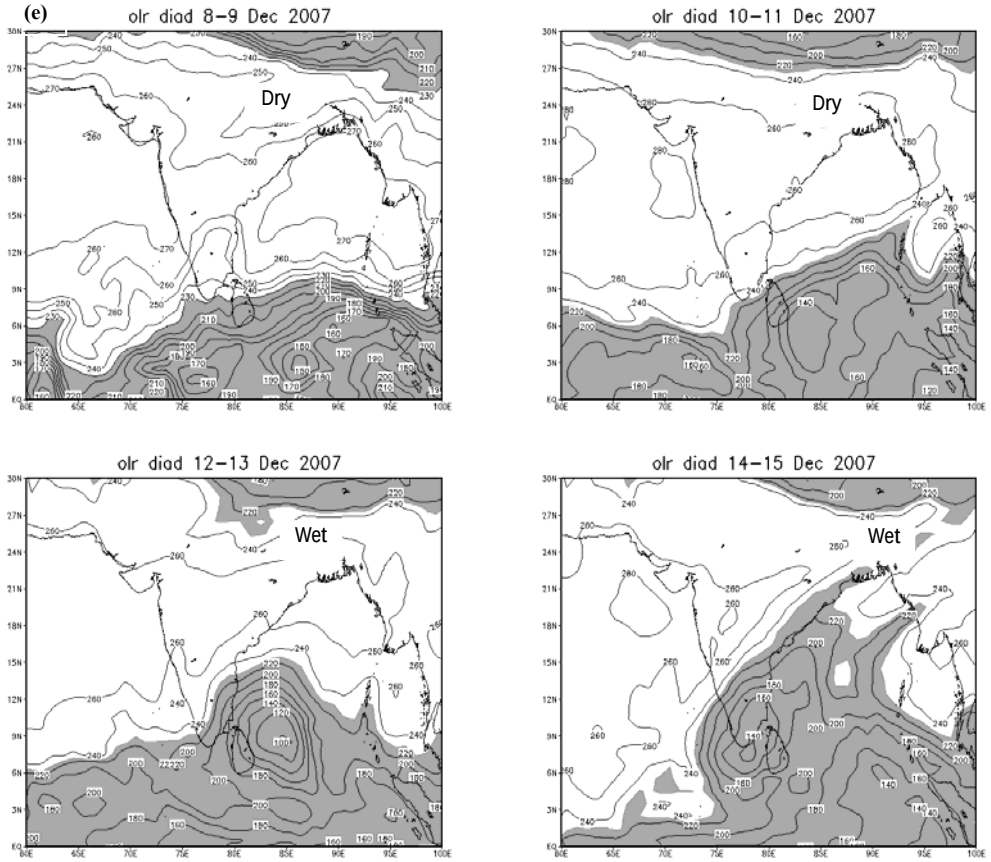

Figs. 7(a-e). Spatial variation in OLR during the years 2001-04 and 2007 when a wet spell of rain followed a prolonged dry spell of northeast monsoon activity (*shaded areas* : OLR ≤ 230 Wm^{-2})

the investigations carried out using such OLR data derived from statistical algorithms. It is interesting to note that despite instrumental and statistical limitations, important characteristics of NEM have emerged in view of the strength of the NEM which marks its presence each year.

In the case of the six spells of remaining five years *viz*., 2001-04 and 2007 and in the second spell of year 2012, where there was no such overlapping of the dry and wet spells with the dates of occurrence of CDs in BoB/NIO, cloud movement from south to north solely under the strength of NEM current could be verified / substantiated as postulated above, from the OLR patterns observed on the dry and wet spell days and listed in Table 2(a). The methodology of analysis is explained as follows:

While performing SEA of the OLR data of the period 2000-12 to bring out normal characteristics of NEM as featured in Section 6.2 above, the noise inherent in the daily data gets smoothened when the data is composited / averaged over 13 years. In the present analysis of active / weak rainfall spells, the OLR data over the grids points of SPI, is averaged either over two (diad) or three (triad) days depending upon the number of dry / wet days pertaining to the spell [Table 2(a)] under consideration. This sort of flexibility in averaging was adopted on a case-by-case basis after thoroughly examining the daily OLR patterns pictorially, to pick out the signals of south to north movement of clouding as postulated above.

Accordingly, the diad / triad means of OLR were computed and the variability in OLR was plotted, analysed and presented for the identified spells of 2001-04, 2007 [Figs. 7(a-e)] and 2012 (Figure not shown). An examination of the figures generated for each year reveals the cloud free conditions during the dry days that precede the commencement of a wet spell with values of OLR between 240 and 270 Wm^{-2} observed over the SPI. For example, let us take the case of the year 2003 shown in Fig. 7(c). Diad (23-24 November) and triad (25-27 November) averaging of the OLR by splitting the dry days of 23-27 November into two periods, depicts contours of

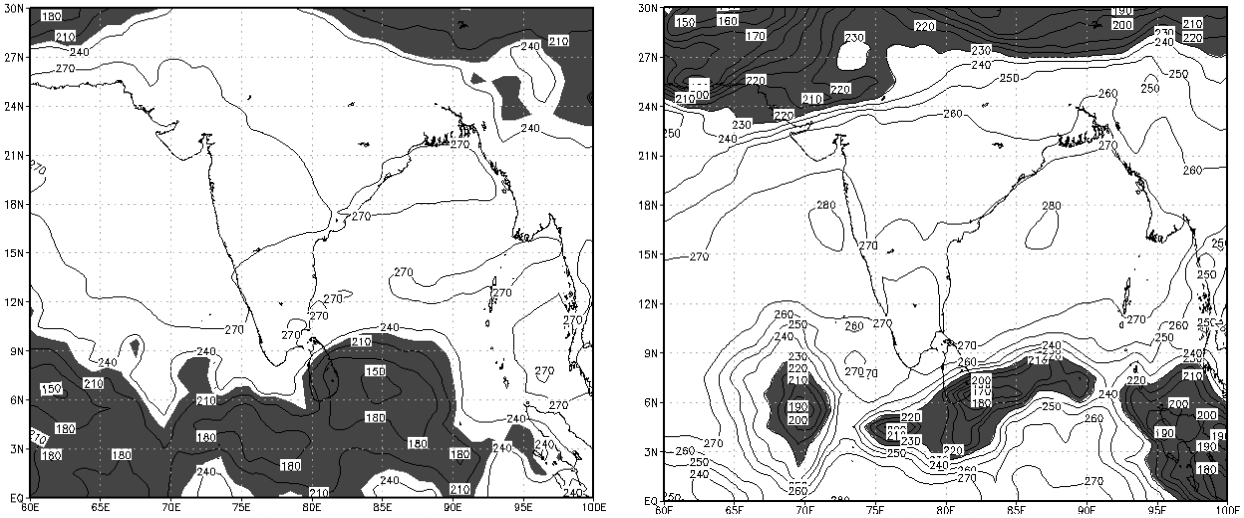

Fig. 8. Spatial distribution of OLR on the dates of withdrawal of northeast monsoon season of the years 2004 and 2007 (*Shaded areas* : OLR ≤ 230 Wm^{-2})

OLR ≥ 230 Wm^{-2} over SPI. The wet spell engulfing SPI with OLR ≤ 230 Wm^{-2} is depicted by the diad means of OLR of 28-29 November and 30 November-1 December. Similar interpretation of OLR patterns is applicable for the rest of the years shown in Figs. 7(a-e). The movement of clouding is consistently from the south/SE/SW direction, with the occurrence of wet spell due to spreading of contours of OLR ≤ 230 Wm^{-2} over SPI. So, irrespective of whether it is a NEM spell during an active onset phase or a post-onset spell when rains commence subsequent to a prolonged dry period, that by and large the clouds approach SPI from south/SE/SW instead of from NE is established firmly. In the case of the years which had the influence of CDs [Table 2(b)] on the wet spells [Table 2(a)] also, the south to north movement of OLR pattern was observed, though such days have not been considered to be representative of the normal strength of NEM current since the effect of the steering winds during CDs dominates the otherwise shallow strength of NEM.

6.4. *Active monsoon over Sri Lanka during withdrawal of NEM from SPI*

Variability in OLR on the dates of withdrawal of NEM for the period 2000-12, was analysed and Fig. 8 is a depiction for the years 2004 and 2007. It is observed in 70% of the years that on the date of withdrawal of NEM, land area between 8-18° N and 73-81° E of SPI is devoid of clouds marking the cessation of RF activity over the region as represented by the presence of isopleths of OLR > 230 Wm^{-2}. Amongst the 13 years, on six occasions, NEM had spilled-over and withdrawn in January of the next year**.** Values of OLR ≤ 210 Wm^{-2} were noticed over parts of Sri Lankan region in almost all the years by the end of December and beginning of January except 2008 and 2012 indicating RF activity congruent to the well established fact that during the withdrawal phase of NEM over TN, Sri Lanka experiences active monsoon conditions. This fact is substantiated by the RF in January over two stations in the northern province of Sri Lanka, *viz*., Mannar (9°00′ N / 79°54′ E) and Jaffna (9°42′ N / 80°00′ E) which receive 65 mm and 70 mm of normal rainfall respectively. Baticaloa (7°42′ N / 81°42′ E) and Trincomalee (8°36′ N / 80°12′ E) both located in the eastern coastal belt receive 265 mm and 180 mm respectively in the month of January (Geetha, 2011). With this information as supportive evidence, a critical and in-depth examination of the pictorial OLR patterns of all days in the second half of December and in January over TN and Sri Lanka was undertaken. The mean OLR was computed for each day of December and January by taking into account the OLRs on the respective dates of all the 13 years (2000-12) over the SPI and the variability was plotted for each day though as a sample Fig. 9 represents only the OLR patterns on 16th & 23rd December, 5th & 28th January. The withdrawal of NEM from TN and the prominent presence of active monsoon conditions and hence RF activity, with values of OLR ≤ 210 Wm^{-2} over Sri Lankan region, adjoining east BoB and NIO is evident from Fig. 9 categorically reaffirming the active phase of monsoon over Sri Lankan region. This result emerging from satellite-derived OLR data, available over NIO, reiterates the observed synoptic feature that monsoon is active over Sri Lankan region during withdrawal of NEM from TN, hitherto characterised only with land based RF data.

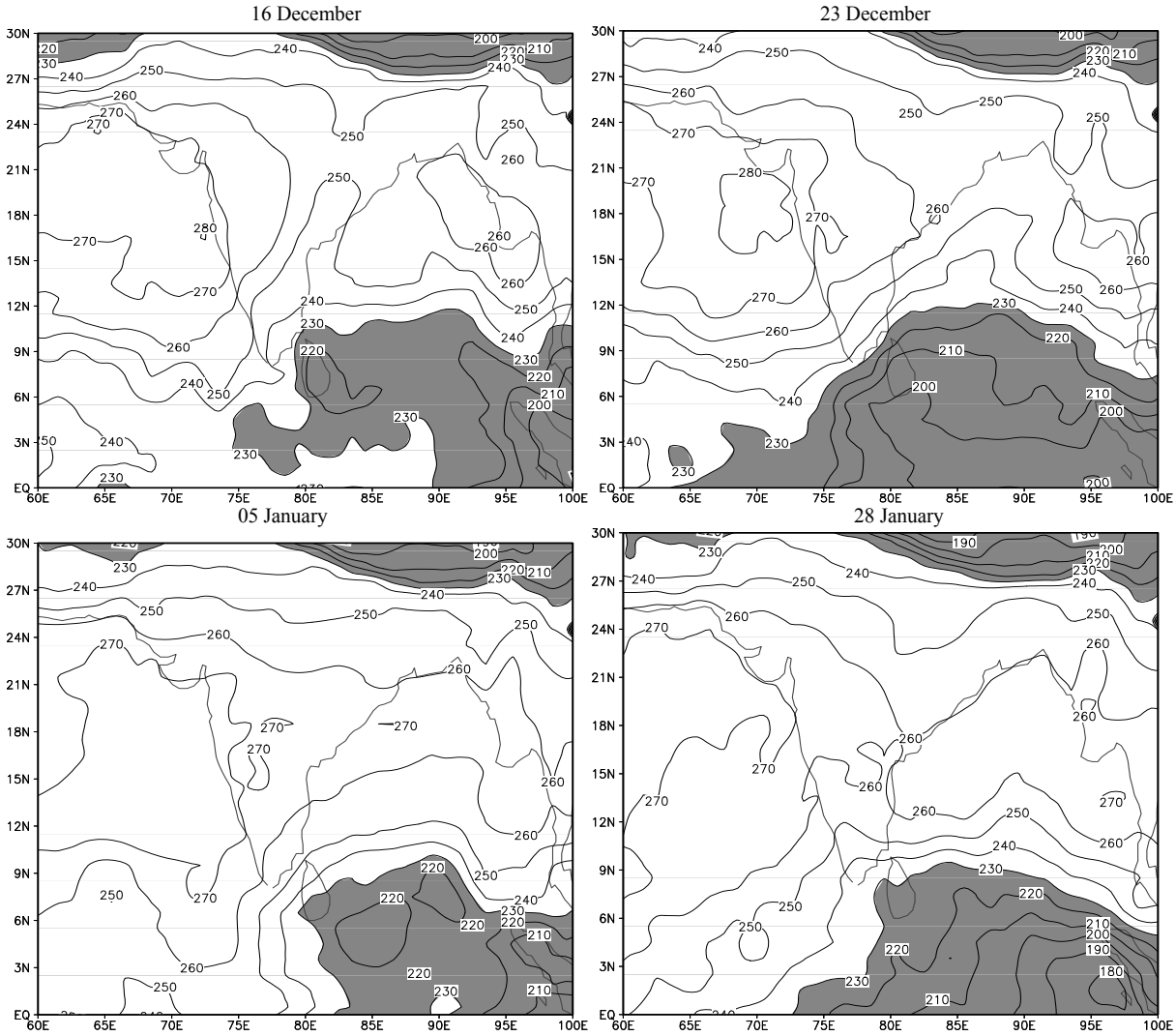

Fig. 9. Mean OLR distribution (2000-12) over Sri Lankan region during the withdrawal phase of northeast monsoon from Tamil Nadu (*shaded areas* : OLR ≤ 230 Wm^{-2})

7. Comments

Overall, the postulate of clouds moving from SE to NW contrary to the expected movement from NE during NEM season when the low level winds are from NE has been verified using satellite-derived OLR data for a comparatively long 26 year period with the present study inclusive. The initial study by Raj *et al.*, *loc. cit.,* for 1987-99, excluding 1992, was based on OLR data of 2.5° × 2.5° resolution. In this study undertaken for the period 2000-2012, OLR data of higher resolution (1° × 1°), has been utilised and the validity of the postulate has been reiterated. Raj, *loc.cit*., have stated that the major mechanisms behind the cloud formation and movement of clouds from south to north are positive relative vorticity in the lower tropospheric level, frictional convergence resulting from land-sea contrast, thermodynamic instability and large amount of moisture flux transported towards coast besides convergence associated with equatorial trough coupled with the prevailing winds and the complex dynamical changes happening in the atmosphere.

Most often, the onset of NEM activity is discerned by the movement of easterly waves of lower amplitude, which approach the south peninsular coast from east. An analytical study of such an easterly wave activity during NEM, 2010 was undertaken by Geetha and Balachandran (2014). Easterly waves can best be tracked through satellite imagery and cannot be easily identified on synoptic charts as they have smaller amplitudes compared to troughs and ridges (Kelkar, 2007). It is most likely that the revival of NEM activity after prolonged dry spells during a particular season, without any visible low

pressure area or a depression may be associated with movement of weaker systems of feeble intensity like that of easterly waves. There is every likelihood that cloud movement associated with an easterly wave is similar to that associated with the movement of a CD, *i.e*., from SE to NW. The results of the analysis using OLR data putforth in the above section bring out the features of a synoptic scale event like NEM with modern data sets.

8. Conclusions

The conclusions derived from this study are listed below:

(*i*) The movement of clouds from south / SE to NW direction during the onset phase of NEM has been reiterated with OLR data of high resolution retrieved from Indian geostationary satellites for the 13 year period 2000-12.

(*ii*) The NLOLR230 taken as the optimal threshold for representing NEM clouding and hence RF, extends eastward up to 18° N, under active NEM conditions. Sometimes it extends even beyond 18° N.

(*iii*) The remnant cloud clusters of SWM, in higher latitudes beyond 27° N were observed on the date of onset of NEM on most of the occasions.

(*iv*) The range in OLR values observed from 90 to 210 Wm^{-2} over NIO / SPI / CTN during 2000-12, on the date of onset of NEM, indicates very intense to good RF activity.

(*v*) Superposed epoch analysis performed on the daily mean OLR data 15 days prior and after the date of onset (total of 31 days) reaffirms the spatial variation and movement of clouds from south towards north at the time of onset of NEM as postulated prior to analysis.

(*vi*) That the movement of clouds is gradually from south / SE towards north / NW / NE could be confirmed through the superposed epoch analysis performed on the OLR data for the period 2000-12 by computing triad and pentad means and assessing the spatial variability of OLR prior to, during and after onset of NEM.

(*vii*) Day-to-day negative OLR anomalies in the range -6 to -4 Wm^{-2} during the pentads of 21-25 and 26-30 October indicate the onset phase of NEM in the south peninsular region. The anomalies otherwise are positive.

(*viii*) The movement of clouding is consistently always from the south/SE directions both during an active NEM onset and a post-onset spell when rain spells (not associated with any moving low pressure area over BoB) commence subsequent to a prolonged dry period.

(*ix*) That a similar type of movement of clouding is observed during the yearly onset of NEM, irrespective of whether the onset is prior to or delayed with reference to the normal date of onset is confirmed.

(*x*) The 13 year period 2000-12 had more number of active spells of NEM than NEM periods of pre-1970s due to the positive RF PDNs which continued for eight NEM seasons during 2004-11. This fact has emerged from the present study.

(*xi*) Since OLR data is available over oceans as well, which is one of the main advantages of satellite-based data retrievals, the inference that the monsoon over Sri Lankan region is active during the withdrawal phase of NEM over TN in the second half of December and in January is another important outcome, conclusively brought out from the spatial OLR variability.

(*xii*) The cloud movement from SE to NW when revival of NEM in the absence of formation of CD over BoB takes place after prolonged dry spells, could possibly be attributed to easterly wave activity and needs further in-depth studies.

Acknowledgement

The authors thank Shri S. B. Thampi, Scientist 'F' & Dy. Director General of Meteorology, Head, RMC Chennai for his unstinted support and Dr. Soma Sen Roy, Scientist 'E', IMD, Pune for the valuable discussions on OLR retrievals. The first author thanks Shri RM. A. N. Ramanathan, Asst. Meteorologist, RMC Chennai for his guidance in using GrADS software.

References

Arkin, A. P., Krishnarao, A. V. R. and Kelkar, R. R., 1989, "Large-scale precipitation and outgoing long wave radiation from INSAT-1B during the 1986 southwest monsoon season", *J. Climate*., **2**, 619-628.

Asokan, R. and Balachandran, S., 2008, "A pre-monsoon precursor for foreshadowing of northeast monsoon rainfall over Tamil Nadu", *Mausam*, **59**, 4, 445-452.

Balachandran, S., Asokan, R. and Sridharan, S., 2006, "Global surface temperature in relation to northeast monsoon rainfall over Tamil Nadu", *J. Earth Syst. Sci*., **115**, 3, 349-362.

Das, P. K., 1986, "Monsoons", IMO lecture, WMO-No. 613.

Geetha, B. and Raj, Y. E. A., 2009, "Role and impact of Siberian High on the temporal variation of Indian northeast monsoon rainfall", *Mausam*, **60**, 4, 505-520.

Geetha, B., Raj, Y. E. A. and Aravindan, V., 2010, "A study of onset phase of northeast monsoon 2009 based on Doppler weather radar echoes", Book of Extended Abstracts, National Seminar on Doppler Radar and Weather Surveillance, DRaWS-2010, 18&19 March 2010, India Meteorological Department, 143-147.

Geetha, B., 2011, "Indian northeast monsoon as a component of Asian winter monsoon and its relationship with large scale global and regional circulation features", Ph.D thesis, University of Madras, Chennai, Chapters 3&9.

Geetha, B. and Balachandran, S., 2014, "An analytical study of easterly waves over southern peninsular India during the northeast monsoon 2010", *Mausam,* **65**, 4, 591-602.

Geetha, B. and Raj, Y. E. A., 2015, "A 140 year data archive of dates of onset and withdrawal of northeast monsoon over coastal Tamil Nadu", *Mausam*, **66**, 1, 7-18.

India Meteorological Department, 1973, "Northeast monsoon", FMU Report No. IV-18.4.

India Meteorological Department, 2008, "Forecasters' Guide", O/o Dy. Director General of Meteorology (Weather Forecasting), Pune, 77.

India Meteorological Department, 2010, "Daily rainfall normals, 1951-2000", CD format, Pune.

India Meteorological Department, 2011, "Cyclone e-Atlas", Version 2, Tracks of cyclones and depressions over north Indian Ocean, Chennai.

Jayanthi, N. and Govindachari, S., 1999, "El Nino and northeast monsoon rainfall over Tamil Nadu" *Mausam*, **50**, 2, 217-218.

Joseph, P. V., Sooraj, K. P. and Rajan, C. K., 2006, "The summer monsoon onset process over south Asia and an objective method for the date of monsoon onset over Kerala", *Int. J. Climatol.,* **26**, 1871-1893.

Kelkar, R. R., Rao, A. V. R. K. and Sant, Prasad, 1993, "Diurnal variation of outgoing long wave radiation derived from INSAT-1B data" *Mausam,* **44**, 1, 45-52.

Kelkar, R. R., 2007, "Satellite Meteorology", B. S. Publications, Hyderabad, ISBN : 81-7800-137-3.

Khole, M. and De, U. S., 2003, "A study on northeast monsoon rainfall over India" *Mausam,* **54**, 2, 419-426.

Kripalani, R. H. and Kumar, Pankaj, 2004, "Northeast monsoon rainfall variability over south peninsular India vis-a-vis the Indian Ocean Dipole Mode", *Int. J. Climatol.,* **24**, 1267-1282.

Kumar, Pankaj, 2006, "Northeast monsoon rainfall prediction", Ph.D Thesis, Pune University.

Mahakur, M., Prabhu, A., Sharma, A. K., Rao, V. R., Senroy, S., Singh, Randhir and Goswami, B. N., 2013, "A high resolution outgoing long wave radiation dataset from Kalpana-1 satellite during 2004-2012", *Curr.Sci.,* **105**, 8, 1124-1133.

Nayagam, L. R., Janardanan, R. and Mohan, H. S. R., 2009, "Variability and teleconnectivity of northeast monsoon rainfall over India", *Global and Planetary Chang*e, **69**, 4, 225-231.

Ohring, G., Gruber, A. and Ellingson, R., 1984, "Satellite determination of the relationship between total long wave radiation flux and infrared window radiance", *J.Clim. Appl. Met.,* **23**, 416-425.

Panofsky, H. A. and Brier, G. W., 1968, "Some applications of statistics to Meteorology", University Press, Pennsylvania, 80-104.

Raj, Y. E. A., 1992, "Objective determination of northeast monsoon onset dates over coastal Tamil Nadu for the period 1901-90", *Mausam*, **43**, 3, 272-282.

Raj, Y. E. A., 1996, "Inter- and intra-seasonal variation of thermodynamic parameters of the atmosphere over coastal Tamil Nadu during northeast monsoon season", *Mausam*, **47**, 3, 259-268.

Raj, Y. E. A., 1998a, "A scheme for advance prediction of northeast monsoon rainfall of Tamil Nadu", *Mausam,* **49**, 2, 247-254.

Raj, Y. E. A., 1998b, "A statistical technique for determination of withdrawal of northeast monsoon over coastal Tamil Nadu", *Mausam,* **49**, 3, 309-320.

Raj, Y. E. A., 2003, "Onset, withdrawal and intraseasonal variation of northeast monsoon over coastal Tamil Nadu, 1901-2000", *Mausam*, **54**, 3, 605-614.

Raj, Y. E. A., Asokan, R. and Revikumar, P.V., 2007, "Contrasting movement of wind based equatorial trough and equatorial cloud zone over Indian southern peninsula and adjoining Bay of Bengal during the onset phase of northeast monsoon", *Mausam*, **58**, 1, 33-48.

Raj, Y. E. A. and Geetha, B., 2008, "Relation between Southern Oscillation Index and Indian northeast monsoon as revealed in antecedent and concurrent modes", *Mausam,* **59,** 1, 15-34.

Raj, Y. E. A., 2012, "Monsoon Monograph", Vol. I, India Meteorological Department, Pune., Ch.13.

Ramage, C. S., 1971, "Monsoon Meteorology", Vol.15, International Geophysics Series, Academic Press, New York and London.

Rao, A. V. R. K., Kelkar, R. R. and Phillip, A. Arkin, 1989,"Estimation of precipitation and outgoing long wave radiation from INSAT-1B radiance data", *Mausam*, **40**, 2, 123-130.

Singh, Randhir, Thapliyal, P. K., Kishtawal, C. M., Pal, P. K. and Joshi, P. C., 2007, "A new technique for estimating outgoing long wave radiation using infrared window and water vapour radiances from Kalpana very high resolution radiometer", *Geophysical Research Letters*, **34**, L23815, doi:10.1029/2007/GL031715.

Suresh, R. and Raj, Y. E. A., 2001, "Some aspects of Indian northeast monsoon as derived from TOVS data", *Mausam*, **52**, 4, 727-732.

Weickmann, K. M., Lussky, G. R. and Kutzbach, J. E., 1985, "Intra-seasonal (30-60 day) fluctuations of outgoing long wave radiation and 250mb stream function during northern winter", *Mon. Wea. Rev*., **113**, 941-961.

Zubair, L. and Ropelewski, C. F., 2006, "The strengthening relationship between ENSO and Northeast monsoon rainfall over Sri Lanka and Southern India", *J. Climate,* **19**, 1567-1575.